GSA Data Repository 2019183

Debris flow processes in southeast Australia linked to the El Niño Southern Oscillation, drought and wildfire: Methods for debris flow mapping, hydro-climatic analyses, rainfall and fire severity analysis and the general additive models, with Figures DR1-DR7 and Tables DR1-DR4

Petter Nyman[1], Ian D Rutherfurd[2], Patrick NJ Lane[1], Gary J Sheridan[1]

[1]School of Forest and Ecosystem Science, University of Melbourne, Parkville, Victoria 3010, Australia

[2]School of Geography, University of Melbourne, Parkville, Victoria 3010, Australia

Contents

Introduction

This supplementary information outlines in more detail the methods and analyses used to address the objectives in the main text.

1. The method of mapping debris flows is outlined. In Fig. DR1, we show examples of channel heads formed at sites runoff- and landslide generated debris flows.
2. Analysis of the association between El Niño Southern Oscillation (ENSO), regional soil moisture, wildfire and extreme rainfall with daily totals (P_{24}) > 150 mm (Fig. DR2). This analysis supports the interpretation of Fig. 2 of the main text.
3. The method for analysing channel head densities are outlined with supporting figures (Fig. DR3-DR6). This part includes a table (Table DR1) with details on site attributes and debris flow surveys at Wilson Promontory (WP), The Grampians (GR), Kilmore-Murrindindi (KM), and Beechworth (BW) that support some of the interpretation of Fig. 4 in the main text.
4. The complete results from the general additive model (GAM) are reported in Table DR2 and Table DR3 as supporting information to the partial dependencies reported in Fig. 3 of the main text.
5. We describe the analysis that supports the interpretation of the slope-area relation in Fig. 4 of the main text. This section provides more details on the methods for identifying valley heads (Eq. DR1 and Eq. DR2; Fig. DR7) and the analyses of the slope-area relation (Fig. 4 in main text).

6. In Table DR4 we report the 30-minute rainfall intensities after wildfire at Wilsons Promontory and The Grampians, where runoff-generated debris flows were not observed.

Debris flow mapping

For runoff generated debris flows in burned areas at Kilmore-Murrundindi and Beechworth we analysed debris flows from the inventory produced in Nyman et al. (2015). Those debris flows were mapped using 15 cm resolution aerial imagery captured in December 2009 and January 2010, 10-11 months after wildfire. Aerial images from March 2009, taken 2-3 weeks after the wildfire, were used as reference images to aid in the identification of channel heads upslope from the fans. Fans were fist located to isolated catchment where debris flow had occurred. Comparison of the aerial imagery interpretation with the field surveys in Nyman et al., (2015) showed that debris flows could be identified with high confidence with a mean accuracy of 0.95 and a precision of 0.89 (true negative rate 0.77; true positive rate 0.94) if deposits were larger than 10 m^2. For deposits with surface area <10 m^2 (typically located in small 1st order headwaters) there was more uncertainty in the observations.

Channel heads above debris flow fans were defined as the starting point of an incision that has a minimum depth of 20 cm (through the A-horizon) over at least 5 meter of channel length. This definition was based on field surveys in past work (Nyman et al., 2011; Nyman et al., 2015) and consistent with definitions of initiation points used elsewhere (Hyde et al., 2007). When compared with field surveys of 51 channel heads, the locations mapped from aerial photography were on average within 19 m ± 3 SE of the location defined from the field survey. This error has very little impact on the slope and area values calculated at the channel heads. For drainage area, this error in channel head location translates to a mean percentage error of ± 4%. For slope, this error in channel head location translates to a mean percentage error of ± 7%. For landslide generated debris flows the location of channel heads were mapped from 15 cm resolution aerial imagery captured within 1 month of the rainfall event that triggered the landslides. Landslides that lead to debris flows were identified and mapped separately from those that terminated without transitioning into a debris flow. The headscarp of the landslide was defined as the channel head. The density of channel heads was calculated for all sites and represented in a 1 x 1 km grid. Table DR1 contains a data summary from all sites. Figure DR1 shows examples of the channel heads for the two debris flow types. Locations of all channel heads are provided in a separate excel file.

ENSO, relative soil moisture and incidence of wildfire and extreme rainfall

Timeseries of relative soil moisture were plotted against the Southern Oscillation Index (SOI) to examine the degree of coupling between the two (Fig. DR2). The relative soil moisture was average over 5-month interval and compared against the 5-month running average of SOI (Fig. DR2 A). This

result shows that on El Niño tends to drier than La Niña, with a significant difference between the two (t=-5.02, df=62, p<0.01). Wildfires leading to runoff generated debris flows occur in periods with drier than normal hydroclimatic conditions (mean =-0.24) which is close to the lowest 25th percentile). Landslides occurred mainly during periods with wetter than usual conditions (0.12) (Figure DR2 A). Differences in moisture condition leading up the events are significant (two sample T-test: p=0.017, df=56, t=-3.26). The cumulative area impacted by extreme rainfall (P_{24} >150 mm) and wildfires indicate that SOI exert a strong control on the two processes (Fig. DR2 B).

Rain intensity and fire severity

For runoff-generated debris flows at Beechworth and Kilmore-Murrundindi the 0.5-hour rainfall totals ($P_{0.5}$) leading debris flows were obtained from analysis of radar data (described in Nyman et al., 2015), where each scan represents 10-minute intensities at a resolution of 0.5 km^2. The intensity estimated from the mean of three consecutive scans were found to correlate reasonably well with measurements from tipping bucket rain gauges (parsons-r= 0.71; n =17) within the two study areas. The half-hourly intensities were averaged into a 1 km grid, which was aligned with the grid of debris flow initiation density. For landslide-generated debris flows at The Grampians and Wilsons Promontory, the daily rainfall (P_{24}) was estimated by spatial interpolation (natural neighbour interpolation) of measured daily totals at gauging stations distributed in and around the study areas. The grid resolution of the interpolated rainfall grids was set to 1 km, aligned with the grid of debris flow initiation density. In The Grampians the interpolated grid was produced from 26 rainfall measurements in an area of 17589 km^2, centred on the 3995 km^2 study area, which contained 8 of the 26 measurements. Measurements outside the study area were used because these remove interpolation artifacts along edges of the study area. At Wilsons Promontory there were 16 measurements across 17422 km^2 centred on the 638 km^2 study area, which contained 4 of the 16 measurement sites.

Fire severity was quantified with the difference Normalised Burn Ration (dNBR) (Key and Benson, 2005), calculated from Band 4 and 7 in pre- and post-fire Landsat images, captured on cloudless conditions 2-3 months before and after the burn. At Beechworth and Kilmore-Murrundindi, the fires burned in February 2009. At Wilsons Promontory, fires burned in the landslide affected area in February 2009 and in April 2006. At The Grampians the landslide affected area was burned in January 2006. The dNBR values, calculated at 30 m resolution, were averaged into a 1 km grid, which was aligned with the grid of debris flow initiation density. Gradient, S [-], was calculated from 10m digital elevation models (DEMs). The proportion of cells with S > 0.3 was calculated in a 1 km grid, which was aligned with the grid of debris flow initiation density. All spatial analyses were done in Matlab. Figures DR3-DR6 show the landscape (Google Earth Image) and the derived spatial data for the four sites used in the analysis.

General additive model (GAM) and partial dependency

Using a generalised additive model (GAM) (Wood, 2017), the data on initiation point density (response) fire severity, slope and rainfall (covariate) were analysed with aim to determine the strength with which independent variables influence debris flow initiation (Table DR2 and DR3). The theory underlying GAMs and the method of fitting models to data is described in Wood (2017). A GAM estimates non-linear relationships with between covariate and the response with thin-plate spline smoothing functions. Thus, the benefit of GAM over general linear models is that the relationship between a covariate and the response variable is not assumed to be linear. Furthermore, when the effects of covariates are additive, it means that the marginal impact of a single variable can be quantified independently from the value of other variables in the model. This marginal impact can be plotted for all covariates in partial dependency plots, which allow for simple interpretations of how predictor variables affect the response variable.

In GAMs there are three parameters that control the level of complexity in smoothing functions and the penalties that avoid overfitting;

- *n_splines*: Number of splines in each of the smooth functions
- *lamda*: A penalization term that is multiplied to the second derivative in the overall objective function.
- *constraints*: Constraints that allows for the inclusion of *a priori* assumptions about the type of relation between a covariate and the response variable. For instance, the relation can be constrained to be convex, concave or monotonically increasing/decreasing.

The models were fit using PoissonGAM in pyGAM (Servén and Brummitt, 2018). A Poisson response distribution is often used with count data and thus suitable for debris flow density, counts the number of events per unit area. The model was fit assuming monotonically increasing debris flow density for all independent variables. Number of splines, *n_splines*, was set to 10. Setting *n_splines* > 10 only marginally improved the fit, while introducing complicated and non-meaningful wiggliness. The penalization parameter, *lamda*, was optimised iteratively to maximized log-likelihood.

Valley head identification and analysis of slope-area curve

Valley heads were identified from the slope of the cumulative area distribution in 8 catchments from which the slope-area data were obtained (Fig. DR7). The position of the valley head was determined objectively by fitting a function to the slope of the CAD and locating the point when the slope was within 5% of the asymptote:

$$slope\ of\ the\ CAD = y + a(1 - e^{-bA)} \quad \text{Eq DR1}$$

Where A is drainage area [m^2] and where y, a and b were fit to the mean slope of the 8 catchments (Fig. DR7). The equation was fit in Matlab using the Levenberg-Marquardt algorithm to data between where the slope of the CAD was at a minimum at low drainage areas (~10^3 m^2) and where the slope of

the CAD was at a maximum (~10^5 m^2). The asymptote of the function is $y + a$. The valley head was defined when the slope of the CAD was within 5% of this asymptote.

The shape of the slope-area data was analysed to determine if the data indicate contrasting geomorphic processes in terms. The non-linear scaling of slope-area data were fit with Eq. 5 from (Stock and Dietrich, 2003):

$$S = \frac{S_0}{1 + a_1 A^{a_2}} \qquad \text{Eq DR2}$$

Where *S* and *A* are slope [-] and drainage area [m^2], respectively. S_0 is the slope at the steepest location on the hillslope (at the inflection point), a_1 is inversely proportional to curvature and a_2 is the power law slope at large drainage areas. Eq DR2 was fit in Matlab using the Levenberg-Marquardt algorithm to all slope-area data downstream from the inflection point. The second derivative of Eq DR2 was used to separate between fluvial and debris flow domain. The value of a_1 was examined to determine the strength of non-linearity in the slope-area scaling and degree with which runoff or mass-failure contribute to landform. A low value of a_1 indicates large curvature, and thus a more distinct break in slope-areas scaling.

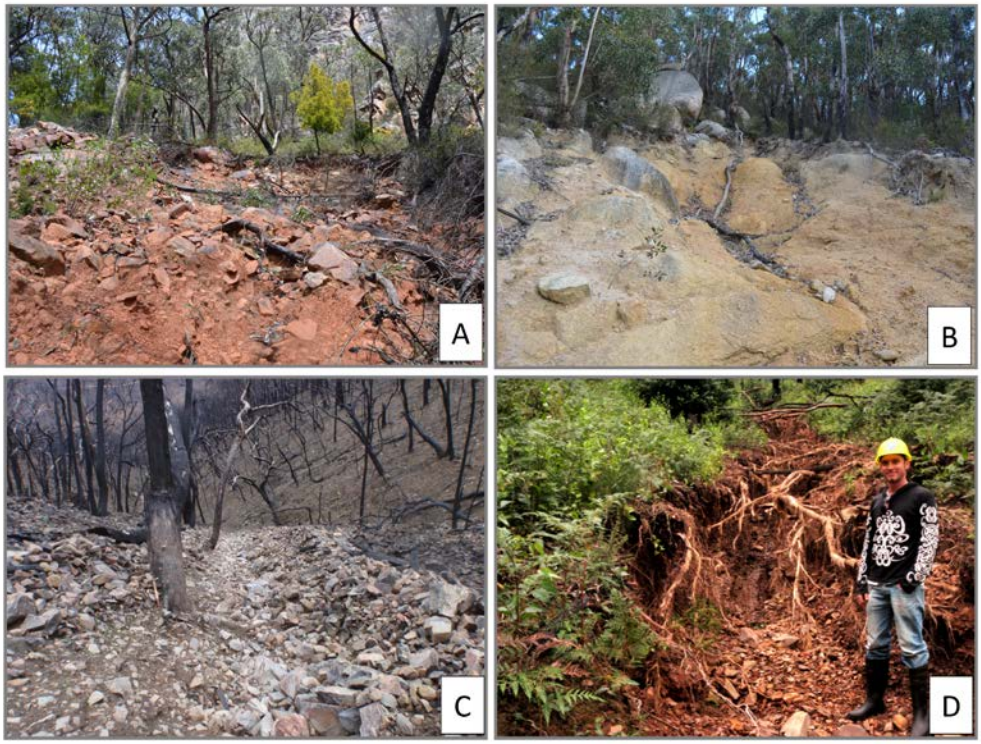

Figure DR1. Channel heads for two debris flow types. A: Channel head for a landslide at The Grampians. B: Channel head for a landslide at Wilson Promontory. C: Channel head formed by runoff-generated debris flow in the Kilmore-Murrindindi fire. D: Channel head formed by runoff-generated debris flow in the Beechworth fire.

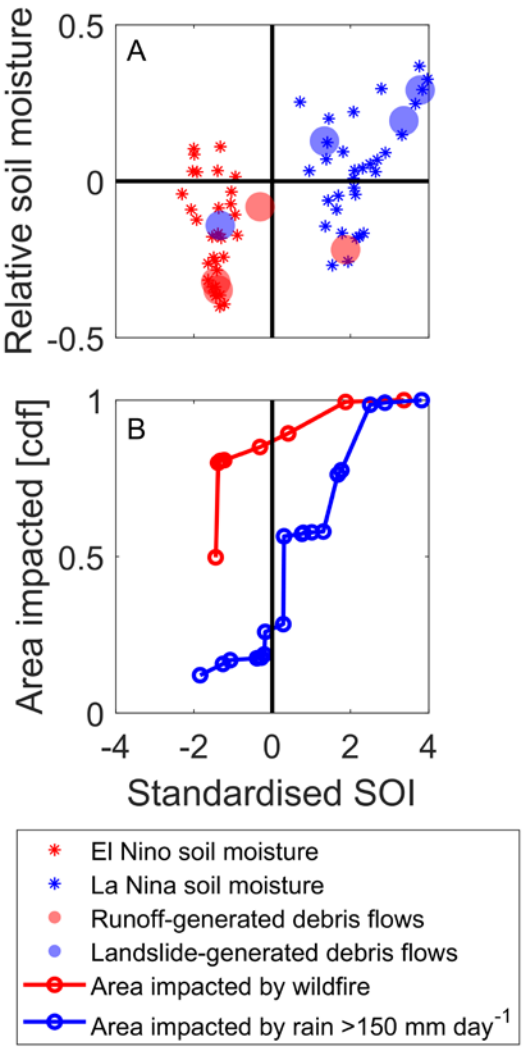

Figure DR2. A: Associations between ENSO, relative soil moisture, debris flows caused by post-wildfire runoff and landslides. B: Cumulative distribution of area impacted by wildfire and rain with P_{24}> 150 mm as a function of SOI.

.

Table DR1. Site attributes and debris flow summaries. The sites are Wilson Promontory (WP), The Grampians (GR), Kilmore-Murrindindi (KM), and Beechworth (BW)

Site [1]	Debris flow trigger	Study area[6]			Dominant landform	Soil type[2]	Soil thick-ness[3]	Texture[4]					Rainfall[5]	Initiation points		Mean slope at channel head	Mean area at channel head	SA relation from Eq 5 in Stock and Dietrich (2003) (Eq DR2)			
		Lat	Lon	km^2			m	Clay %	Silt %	Fine & medium sand %	Coarse sand %	Gravels %	mm	n=	per km^2	S_{df} m m^{-1}	A_{df} m^2	s_0 m m^{-1}	a_1 $*10^{-4}$	a_2	R^2
WP	Landslide	-39.0	146.4	638	Dissected granite	Duplex soil	0.90	3	19	15	31	32	215-372	179	0 - 16	0.56	$4.9*10^3$	0.52	3.91	0.68	0.98
GR	Landslide	-37.3	142.5	3995	Marine sedimentary cuesta	Shallow stony sands	0.65	5	25	30	19	21	51-146	139	0 - 11	0.68	$4.8*10^3$	0.53	0.55	0.84	0.99
KM	Runoff	-37.4	145.4	3256	Dissected marine sedimentary	Shallow stony earths	0.60-0.90	14	22	20	1	43	0 - 61	445	0 - 8	0.29	$7.6*10^4$	0.50	6.47	0.70	0.99
BW	Runoff	-36.5	146.8	1107	Dissected marine sedimentary	Friable earths	0.30-1.00	13	20	17	6	43	2 - 35	125	0 - 9	0.34	$2.4*10^4$	0.47	2.97	0.70	0.99

[1]GR=Grampians; WP=Wilson's Promontory; KM=Kilmore Murrindindi; BW=Beechworth

[2]Soil type defined according to Northcote (1971) and obtained from "LSYS250 State wide soil attribute coverage" DOI 10.4226/92/58e727e0dd1. Accessed November 21, 2018.

[3] Soil thickness from "GMU250 - Geomorphology units of Victoria". DOI:10.4226/92/58e6f2752cfd6. Accessed November 21, 2018.

[4]Soil texture measured using laser particle sizer on samples collected in soil cores from colluvium at channel heads. The number of channel heads sampled were 5, 4, 2 and 4 for WP, GR, KM and BW respectively. At each channel head soil cores were obtained on two profiles at 3 depths. Values are the average for each site.

[5]Range of rainfall in 1 km x 1 km cells where debris flows were observed.

[6]Latitdue and longitude are the centre of the domain as shown in Figures DR3-DR6

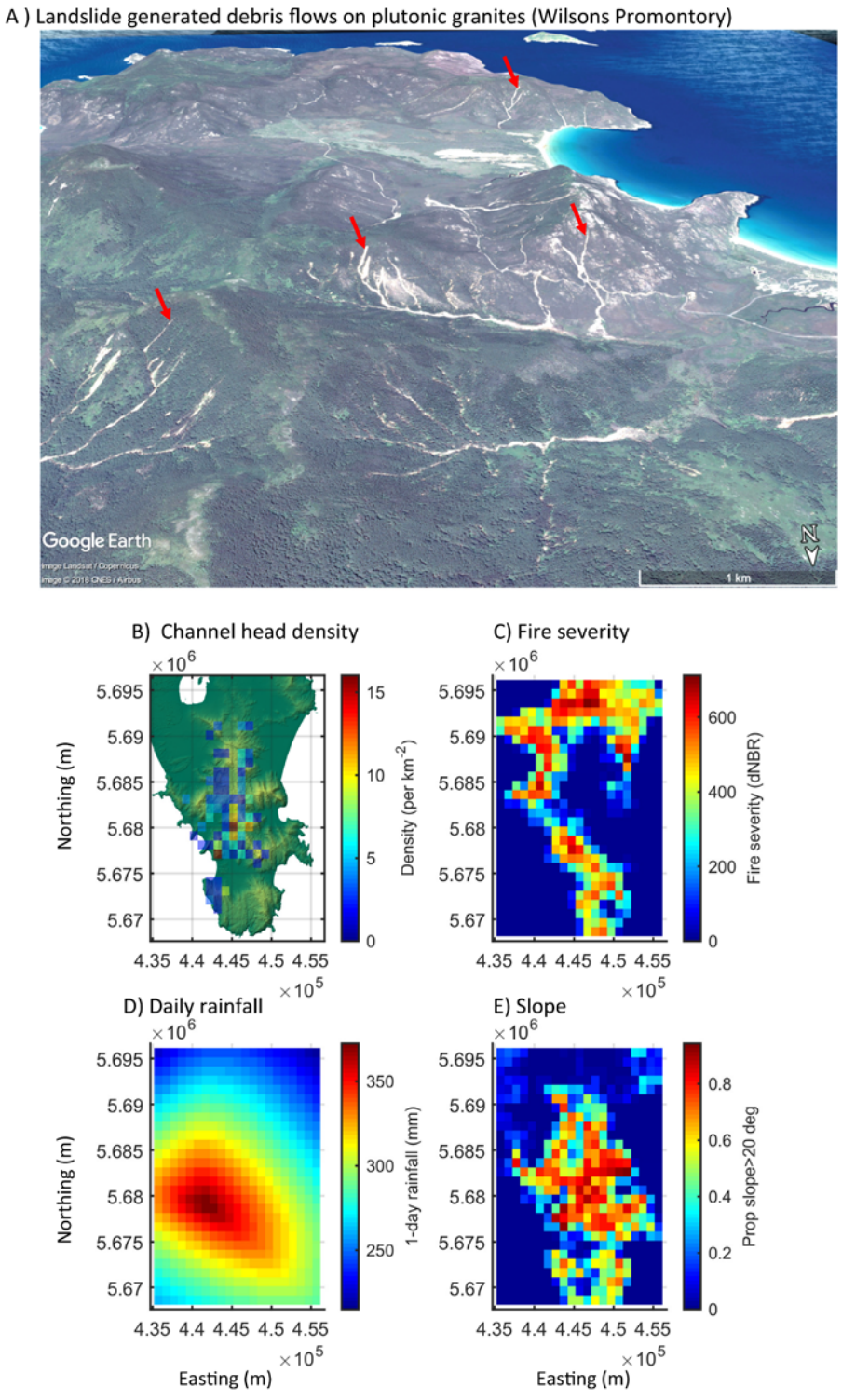

Figure DR3. A: Landscape setting at Wilsons Promontory (WP) and some examples of channel heads marked with red arrow. B: Channel head density with terrain model. C: Fire severity. D: Daily rainfall. E: The proportion of area with gradient > 0.3.

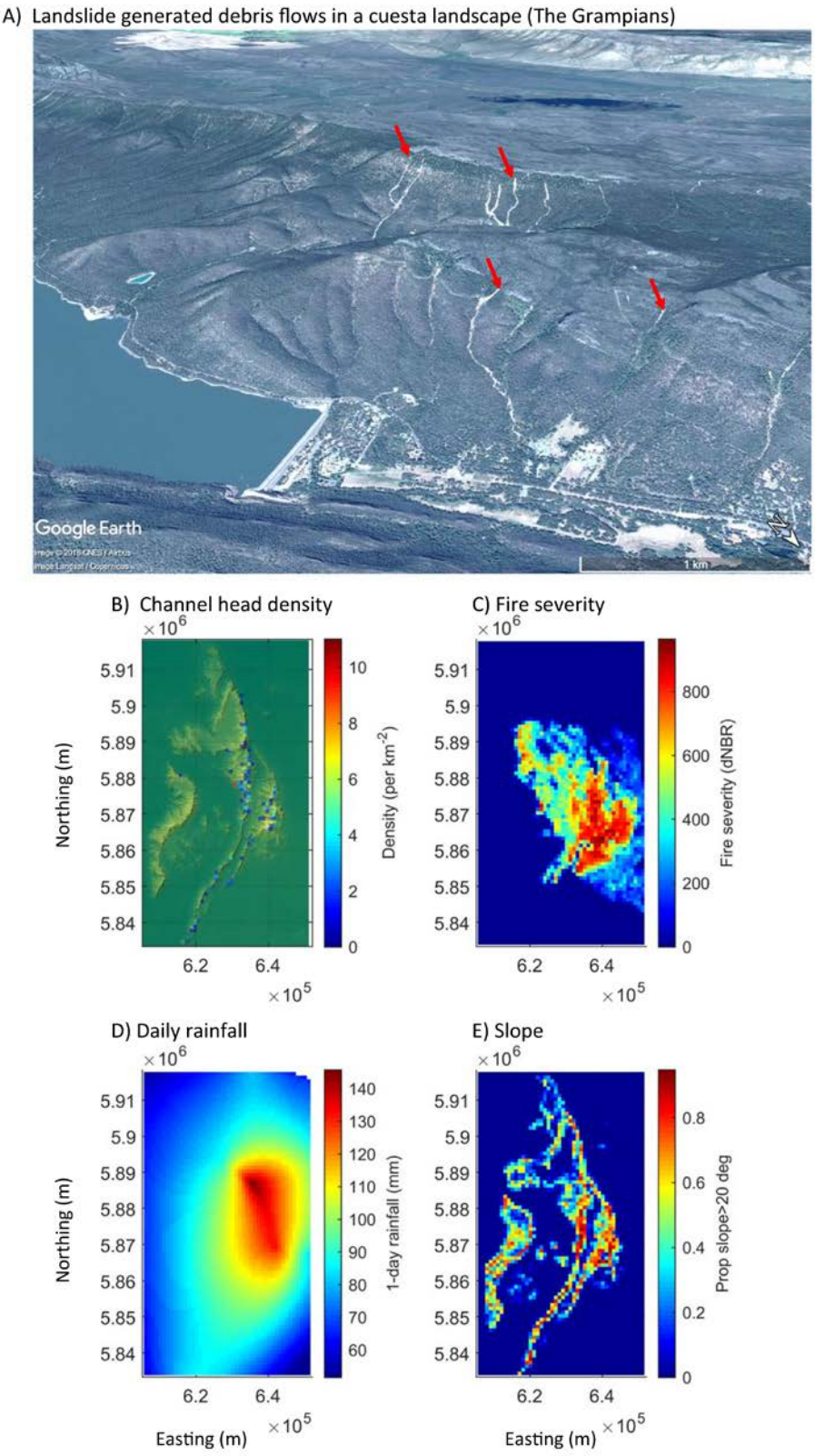

Figure DR4. A: Landscape setting at The Grampians (GR) and some examples of channel heads marked with red arrow. B: Channel head density with terrain model. C: Fire severity. D: Daily rainfall. E: The proportion of area with gradient > 0.3.

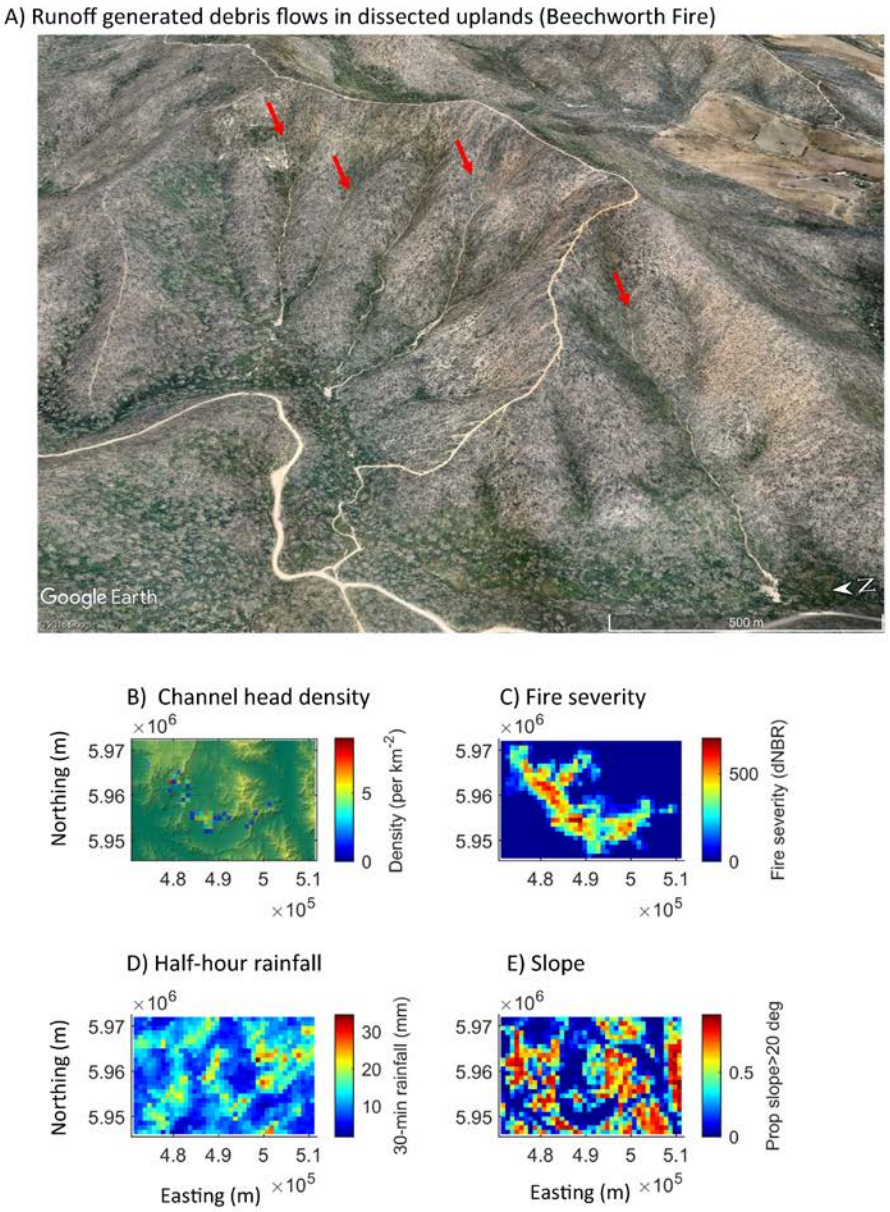

Figure DR5. A: Landscape setting at the Kilmore - Murrindindi Fire (KM) and some examples of channel heads marked with red arrow. B: Channel head density with terrain model. C: Fire severity. D: Half-hourly rainfall. E: The proportion of area with gradient > 0.3.

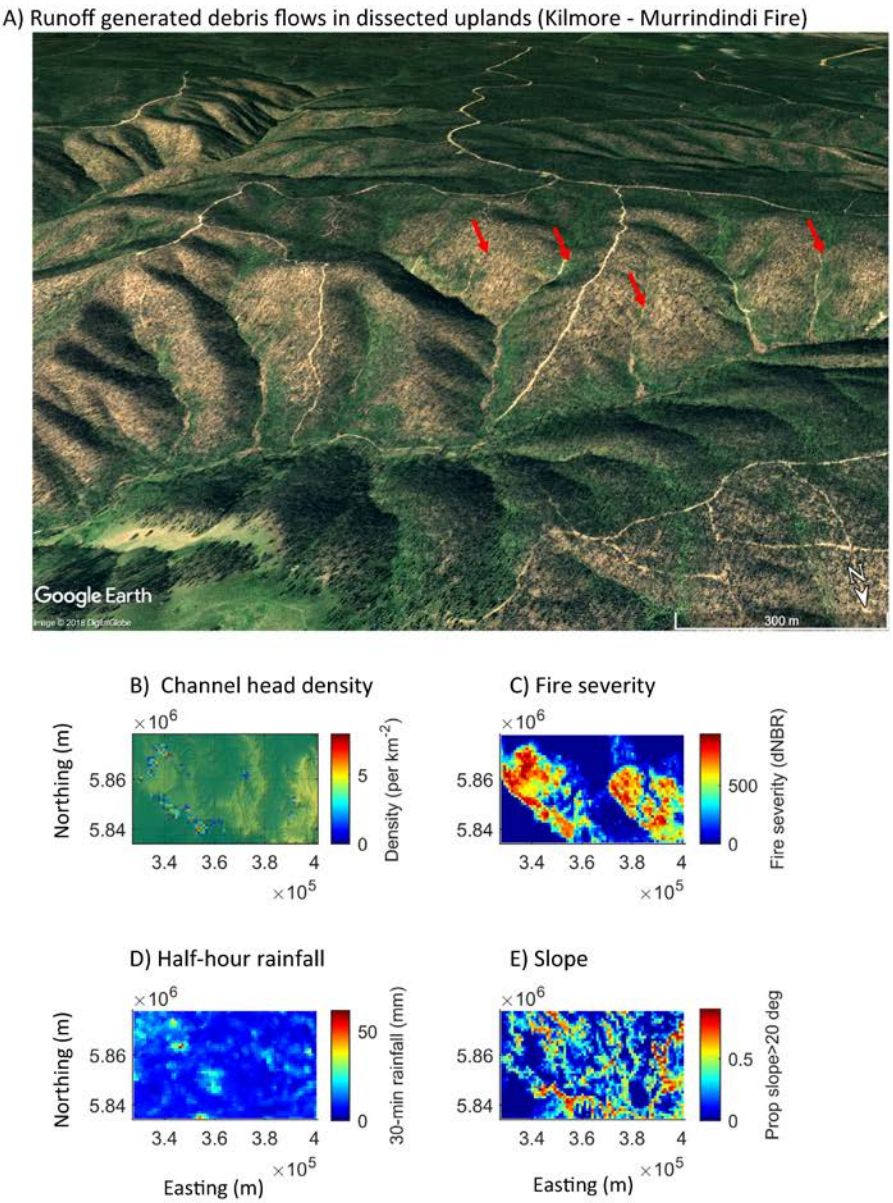

Figure DR6. A: Landscape setting at the Beechworth Fire (KM) and some examples of channel heads marked with red arrow. B: Channel head density with terrain model. C: Fire severity. D: Half-hourly rainfall. E: The proportion of area with gradient > 0.3.

Table DR2. Generalised additive model (GAM) fit to a Poisson distribution of initiation density in landslide generated debris flows (LGDF)

Distribution:	PoissonDist	Effective DoF:	9.4105
Link Function:	LogLink	Log Likelihood:	-861.916
Number of Samples:	4427	AIC:	1742
		Un-biased Risk Estimator:	2.30
		Deviance:	0.64

Feature	Data Type	Splines	Lambda	P-value[1]
Slope	numerical	10	0.2512	0
dNBR	numerical	10	0.2512	$8.44*10^{-5}$
Rainfall	numerical	10	0.2512	0
Intercept	intercept			0

[1]When smoothing parameters have been estimated, the p-values are typically lower than they should be, meaning that the tests reject the null too readily. This is because smoothing parameter uncertainty has been neglected in the reference distributions used for testing (Wood, 2017).

Table DR3. Generalised additive model (GAM) fit to a Poisson distribution of initiation density in runoff generated debris flows

Distribution:	PoissonDist	Effective DoF:	13.5834
Link Function:	LogLink	Log Likelihood:	-1199.12
Number of Samples:	4319	AIC:	2425.403
		Un-biased Risk Estimator	2.44
		Deviance	0.51

Feature	Data Type	Splines	Lambda	P-value[1]
Slope	numerical	10	0.004	0
dNBR	numerical	10	0.004	0
Rainfall	numerical	10	0.004	$4.8*10^{-7}$
Intercept	intercept			$3.9*10^{-8}$

[1]When smoothing parameters have been estimated, the p-values are typically lower than they should be, meaning that the tests reject the null too readily. This is because smoothing parameter uncertainty has been neglected in the reference distributions used for testing (Wood, 2017).

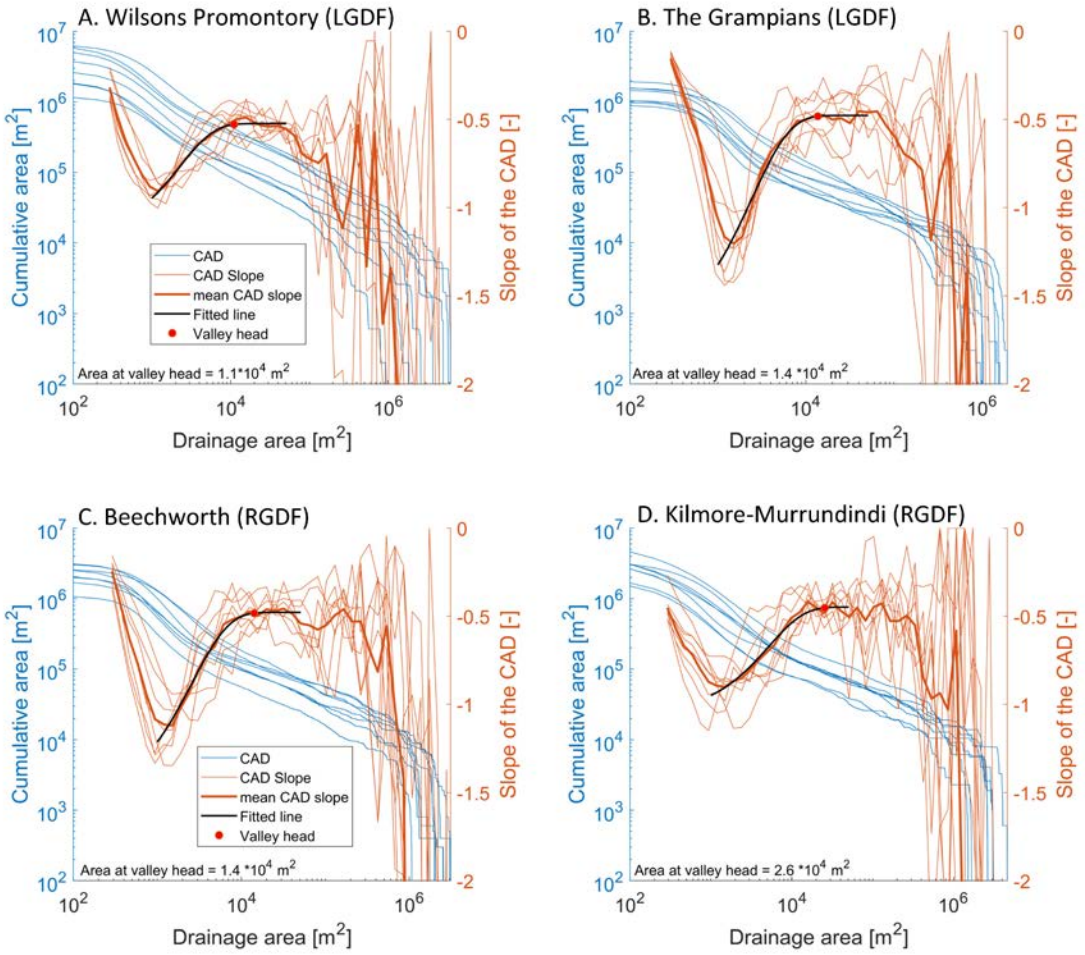

Figure DR7. Cumulative area distribution (CAD) and slope of the CAD. A: Wilsons Promontory. B: The Grampians. C: Beechworth. D: Kilmore-Murrundindi.

Table DR4. Peak 30-minute rainfall intensities at Wilsons Promontory and The Grampians in the first 2 years after wildfire.

Site	Weather station	Location		Time since fire	30-minute rainfall intensity ($P_{0.5}$)
		Lat	Lon	Months	mm hr^{-1}
Wilson Promontory	Wilson Promontory Lighthouse	-39.1297	146.4244	15	35.2
				14	34.0
				8	28.0
				1	24.0
				5	21.6
The Grampians	Grampians (Mt William)	-37.295	142.6039	15	26.4
				16	24.8
				12	23.6
				12	20.0
				13	19.6

REFERENCES

Hyde, K., Woods, S.W., and Donahue, J., 2007, Predicting gully rejuvenation after wildfire using remotely sensed burn severity data: Geomorphology, v. 86, no. 3-4, p. 496-511, doi:10.1016/j.geomorph.2006.10.012

Key, C.H., and Benson, N.C., 2005, Landscape Assessment: Ground measure of severity, the Composite Burn Index; and Remote sensing of severity, the Normalized Burn Ratio: USDA Forest Service, Rocky Mountain Research Station, USDA Forest Service General Technical Report, RMRS-GTR-164-CD, 55 p.

Northcote, K.H., 1971, Factual key for the recognition of Australian soils: Glenside, Australia, Rellim Technical Publications Pty., 123 p.

Nyman, P., Sheridan, G.J., Smith, H.G., and Lane, P.N.J., 2011, Evidence of debris flow occurrence after wildfire in upland catchments of south-east Australia: Geomorphology, v. 125, no. 3, p. 383-401, doi:10.1016/j.geomorph.2010.10.016

Nyman, P., Smith, H.G., Sherwin, C.B., Langhans, C., Lane, P.N.J., and Sheridan, G.J., 2015, Predicting sediment delivery from debris flows after wildfire: Geomorphology, v. 250, p. 173-186, doi:http://dx.doi.org/10.1016/j.geomorph.2015.08.023

Servén, D., and Brummitt, C., 2018, pyGAM: Generalized Additive Models in Python, https://github.com/dswah/pyGAM.

Stock, J., and Dietrich, W.E., 2003, Valley incision by debris flows: Evidence of a topographic signature: Water Resources Research, v. 39, no. 4, p. 1089, doi:10.1029/2001WR001057

Wood, S.N., 2017, Generalized additive models: an introduction with R: New York, Chapman and Hall/CRC, 406 p.